

Laponite-Based Surfaces with Holistic Self-Cleaning Functionality by Combining Antistatics and Omniphobicity

*Marta Fenero,^a Jesús Palenzuela,^{*a} Itxasne Azpitarte,^b Mato Knez,^{b,c} Javier Rodríguez,^a and
Ramón Tena-Zaera^a*

^aIK4-CIDETEC, Parque Tecnológico de San Sebastián, Paseo Miramón, 196, 20014 Donostia -
San Sebastián, Spain.

^bCIC nanoGUNE, Tolosa Hiribidea, 76, 20018 Donostia - San Sebastián, Spain.

^cIkerbasque, Basque Foundation for Science, Maria Díaz de Haro 3, 48013 Bilbao, Spain

KEYWORDS: Self-cleaning, omniphobicity, antistatics, dust-repellency, laponite

ABSTRACT: In the present work, perfluoroalkylated laponite nanoparticles with a high degree of functionalization (60 wt%) have been prepared and a methodology to prepare transparent, antistatic and omniphobic laponite-based films with holistic self-cleaning properties against liquids, solids and liquid-solid mixtures has been developed. The intrinsic electrical and ionic conductivities observed in unmodified laponite coatings are combined with perfluoroalkyl-modified laponite clays. As a result, films with improved self-cleaning functionality based on dust-repellency and omniphobic liquid-repellence (sheet resistance in the range of $10^7 \Omega/\square$ and

1
2
3 contact angles of 106° (H₂O) and 93° (oil)) were obtained. These unique films, being capable to
4
5
6
7
8
9
10
11
12
13
14
15
16
17
18
19
20
21
22
23
24
25
26
27
28
29
30
31
32
33
34
35
36
37
38
39
40
41
42
43
44
45
46
47
48
49
50
51
52
53
54
55
56
57
58
59
60

contact angles of 106° (H₂O) and 93° (oil)) were obtained. These unique films, being capable to
repel dust and liquids, were applied to a variety of substrates (i.e. glass and plastics) and tested
against solids and liquids of different nature with excellent performance. Bending tests of these
holistic self-cleaning films deposited over flexible substrates showed better mechanical
performance than unmodified laponite films.

1. INTRODUCTION

Self-cleaning coatings have attracted recently a great recognition in research and industry, due to
their great importance for numerous commercial applications, facilitating the daily life of the
society and saving time and money by enabling novel and improved products and technologies.¹⁻

³ The concept of engineering self-cleaning surfaces is inspired by nature, typically by adapting
examples from flora and fauna.⁴ In both natural and engineered systems, the presence of water is
essential. Namely, water droplets roll along a non-wetting surface, thereby collecting dirt
particles and consequently cleaning the surface along their path.⁵⁻⁷ However, hydrophobic or
superhydrophobic surfaces (water contact angles greater than 150° and sliding angles below 10°)
do not provide a self-cleaning response in dry conditions or with liquids dissimilar to water. As a
consequence, droplets of liquids with low surface tension, such as oils or organic solvents,
remain pinned to the surfaces, causing an unaesthetic and stained appearance. Omniphobic
surfaces are defined as surfaces with the ability to repel liquids, regardless their chemical nature,
polarity, or surface tension, hence unifying hydrophobic and oleophobic⁸ characteristics.⁹⁻¹¹
Engineered omniphobic surfaces ideally will repel any kind of liquid and thus remain cleaner
than either of the conventional hydrophobic or oleophobic surfaces. However, the self-cleaning

1
2
3 concept applies only partly to omniphobic surfaces, since the concept it is limited to surfaces that
4 allow rolling droplets and does not provide any self-cleaning response when the surfaces are
5 covered by dust in dry conditions.
6
7
8
9

10
11 An alternative approach to avoid dust accumulation relies on the reduction of the electrical
12 surface resistance, leading to antistatic characteristics, thereby diminishing the dust attraction to
13 the surface.^{12,13} Great efforts are invested in developing antistatic dust-repellent coatings for
14 applications in industrial sectors such as automotive, construction or photovoltaics. Antistatic
15 coatings are also implemented by the industry to elude charge accumulation and dramatic
16 discharges producing dangerous sparks, which may cause equipment failures or fires.^{14,15}
17
18
19
20
21
22
23
24
25

26 However, dust-repellent surfaces have rarely been studied in view of omniphobicity for
27 providing full self-cleaning characteristics and avoiding accumulation of dust and liquids.
28
29 Indeed, to the best of our knowledge, there are no reports on holistic self-cleaning approaches
30 based on such unique combination. Laponite nanoparticles, a synthetic type of silicate nanoclay
31 in the smectite family, show great promise for achieving this holistic approach for the following
32 reasons: 1) laponite particles have intrinsically ionic and electrical conductivity, which could
33 induce antistatic and dust-repellency effects; 2) like other clays, laponites can be flexibly
34 modified through functionalizing the accessible hydroxyl groups,¹⁶ and silanized with
35 omniphobic and fluorinated groups; 3) laponite nanoparticles are easily dispersed in solvents,
36 such as water,^{16,17} and processed to homogeneous and continuous films by conventional coating
37 methods such as casting, bar-coating, dip-coating, or blade-coating¹⁸ and finally, 4) laponite
38 films are typically highly optically transparent.^{19,20} Further properties of laponite coatings
39 include corrosion protection of metals, by preventing the contact of various species, such as
40 water and ions with the metal substrate.^{21,22}
41
42
43
44
45
46
47
48
49
50
51
52
53
54
55
56
57
58
59
60

1
2
3 In this paper, laponite nanoparticles are modified with perfluorinated pendant groups. The
4
5 physico-chemical properties of the modified laponites are characterized and correlated to the
6
7 electrical sheet resistance and omniphobic response. Furthermore, innovative coatings (i.e. based
8
9 on a controlled mixture of unmodified and modified laponites) with dual-action, anti-dust
10
11 accumulation and liquid repellence, are proposed for a holistic approach with a threefold active
12
13 self-cleaning response against liquids, solids and liquid-solid mixtures.
14
15
16
17
18
19
20
21

22 2. EXPERIMENTAL SECTION

23 24 25 **Materials**

26
27
28 Laponite grades XLG and JS from Rockwood Additives Ltd. were kindly provided by Azelis and
29
30 Comindex, respectively. Laponite is a uniform disc-shaped synthetic clay with disc diameters of
31
32 25 nm and thicknesses of 1 nm. 1H,1H,2H,2H-perfluorooctyltriethoxysilane 97% was acquired
33
34 from aber GmbH. Ethanol absolute was purchased from Sigma-Aldrich. All chemicals were used
35
36 as received. Deionized water with a conductivity $< 1 \mu\text{S}$ was used in all experiments. Glass
37
38 substrates with 1 mm thickness were obtained from Deltalab S.L. with reference D100001 and
39
40 cut into 25 x 25 mm squares. PVC substrates with thicknesses of 180 μm were acquired from
41
42 Fellowes and cut into 25 x 25 mm squares.
43
44
45
46
47

48 49 **Synthesis of perfluoroalkylsilanized-modified laponites**

50
51
52 The general procedure for the silanization of laponites has been described previously by other
53
54 authors,^{23,24} however, the methodology was modified and adapted to our materials and target
55
56 product. To a 100 mL round-bottomed flask with 25 mL of deionized water, Laponite XLG (1 g)
57
58
59
60

1
2
3 was added in small portions under vigorous stirring until full dispersion of the solid was
4
5 achieved. After 1 h of stirring, 25 mL of absolute ethanol was added to the clear dispersion,
6
7 followed by the addition of 1H,1H,2H,2H-perfluorooctyltriethoxysilane (1.77 mL). Upon silane
8
9 addition, the solution turned cloudy and was allowed to stir at 50 °C for further 16 h. The cloudy
10
11 white dispersion was collected in centrifuge tubes and centrifuged at 3500 rpm for 20 min. The
12
13 supernatant was decanted and the remaining gel collected and dispersed again in a mixture of
14
15 50% ethanol/water. The centrifuge procedure was repeated to remove all unbound material.
16
17 Finally, the collected gelled clay was redispersed in a total volume of 25 mL of a mixture of 50%
18
19 ethanol/water, leading to a 4% (w/v) dispersion based on the initial laponite amount.
20
21
22
23
24

25 **Substrate preparation**

26
27
28 Before use, the glass substrates were immersed in warm acetone, cleaned with soap and rinsed
29
30 with deionized water in that sequence. PVC substrates were cleaned with soap, rinsed with
31
32 deionized water and activated using a nano Dieder plasma system, consisting of a RF signal
33
34 generator (40 kHz, 200 W). The PVC substrates were exposed to a vacuum of 0.3 mbar before
35
36 treatment with oxygen plasma during 60 s at 90% power to promote adhesion.
37
38
39
40

41 **General procedure for the film fabrication**

42
43
44 Films were prepared by processing the corresponding solution through a bar-coating
45
46 methodology as depicted in Figure 1. The films were prepared by placing the substrates in the
47
48 bar-coating equipment (Sheen 1137-G-MAN automatic film applicator) and applying the
49
50 corresponding solution using a rod-shaped 100 µm size wire coil bar at a speed of 50 mm/s at
51
52 room temperature. After the solution was spread over the substrate, the obtained films were dried
53
54 in an oven at 80 °C during 1 h.
55
56
57
58
59
60

Fabrication of unmodified-laponite films with antistatic functionality

In a 50 mL flask with 25 mL of deionized water, 700 mg of laponite XLG were added in small portions under vigorous stirring. Once the solid was completely dispersed, 300 mg of laponite JS were added in the same manner. The solution turned cloudy. After stirring for 3 h, the solution became clear and a 4% (w/v) XLG:JS (7:3) laponite dispersion, based on the total weight of laponite, obtained. The aqueous laponite dispersion was aged for 2 weeks. The laponite mixture and aging was performed in order to reach a suitable viscosity (circa 8000 cP, shear rate 2.2 s^{-1}) before processing through a bar-coating technique, following the general procedure.

Fabrication of holistic multifunctional laponite films

For the preparation of multifunctional laponite films with self-cleaning synergetic functionalities, a multifunctional laponite mixture 4% (w/v) was initially prepared. Hence, 7 g of the laponite XLG:JS (7:3) 4% (w/v) dispersion from the unmodified laponite solution were taken and mixed with 3 g of the 4% (w/v) perfluoroalkylsilanized-modified laponite solution. The obtained mixture was applied to the substrates through a bar-coating technique following the general procedure. For convenience, the films obtained from the latter mixture are named “multifunctional” throughout the remainder of the manuscript.

Modified laponites and thin film characterization

Fourier transform infrared spectra (FT-IR) of the solids were obtained applying the Attenuated Total Reflectance (ATR) technique with a Jasco 4100 FTIR. The spectra were recorded in the range between 400 cm^{-1} and 4000 cm^{-1} .

1
2
3 Thermal gravimetric analysis (TGA) was carried out on a TA instruments Q500 thermobalance.
4
5 Samples were heated at a rate of 10 °C/min from ambient temperature to 700 °C under a nitrogen
6
7 flow of 60 mL/min.
8
9

10
11 Morphological properties of the film were analyzed using ULTRA plus ZEISS field emission
12
13 scanning electron microscope (FE-SEM).
14
15

16
17 UV-vis spectra were obtained in transmission/absorption mode with a Jasco V-570
18
19 spectrophotometer using air as background. The spectra were recorded between 300 nm and 800
20
21 nm using a film holder accessory for solid samples. Reflectance was measured in the same
22
23 wavelength range using an integrating sphere Jasco ISN-470.
24
25
26

27
28 Sheet resistance of the films was measured at atmospheric pressure and room temperature
29
30 conditions using a Keithley Semiconductor Characterization System 4200-SC with a four-point
31
32 probe.
33
34

35
36 KSV CAM 200 Optical contact angle meter was used to determine the static contact angles of
37
38 the films. Solvent droplets were placed at a minimum of three different areas of each surface.
39
40 The static contact angles were recorded using the Laplace-Young fitting method.
41
42
43
44
45
46
47
48
49
50
51
52
53
54
55
56
57
58
59
60

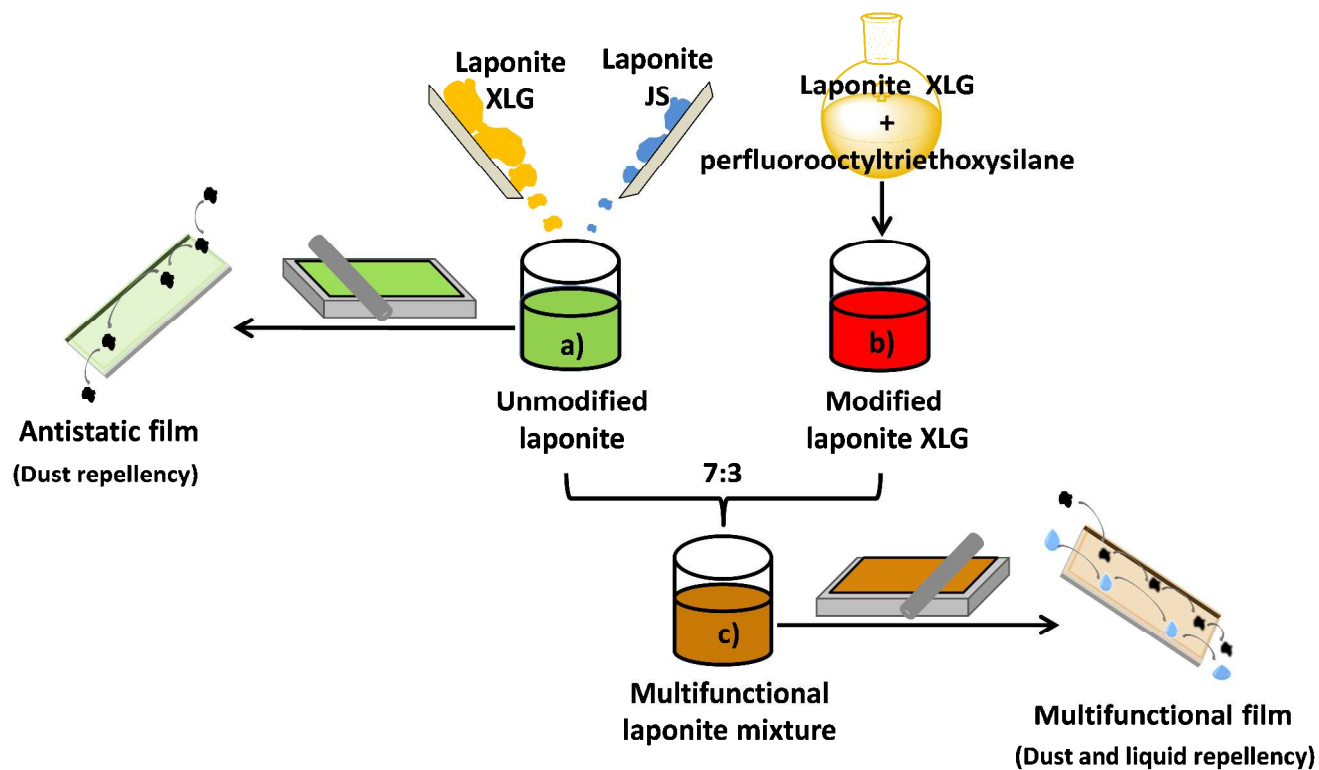


Figure 1. Schematic illustration of the preparation procedure of multifunctional films with self-cleaning response, repelling liquids and dust particles.

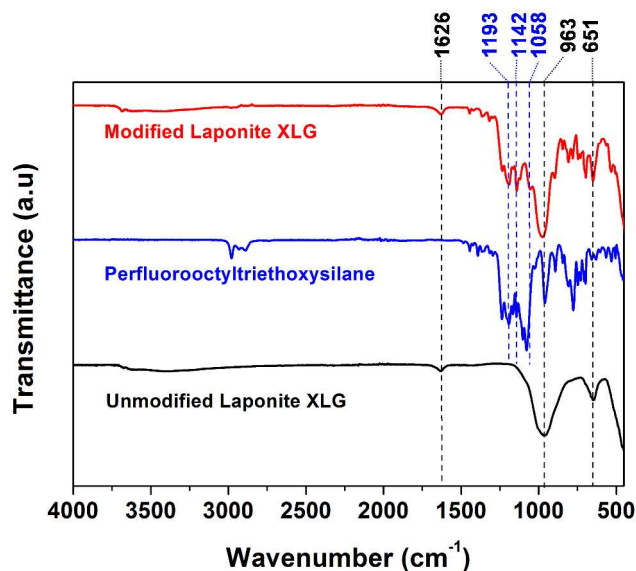
3. RESULTS AND DISCUSSION

Perfluoroalkylsilane-modified laponites

Each laponite nanodisc is known to have an overall negative charge of approximately 700 electron charges,²⁵ which very effectively facilitate the nuclear substitution at the perfluoroalkylsilane to generate new O-Si bonds during the laponite modification process.

Qualitative evidence of the modification was provided by Fourier transform infrared spectroscopy (FTIR). The FTIR spectrum of bare and modified XLG laponite is shown in Figure 2. It is worth noting that the FTIR spectrum of modified laponite showed a clear overlap with the

1
2
3 bare laponite and the silane reagent peaks. According to similar assignments in earlier studies,²⁶
4
5 vibrations of the modified laponite XLG at 651 cm^{-1} and 963 cm^{-1} can be attributed to bending
6
7 and asymmetric stretching of Si-O-Si bonds. Bands between 1000 - 600 cm^{-1} are likely due to C-
8
9 C stretching modes. The presence of C-F groups is obvious from the intense absorption peak
10
11 C stretching modes. The presence of C-F groups is obvious from the intense absorption peak
12
13 around 1058 cm^{-1} . Characteristic bands of CF_2 and CF_3 were found at 1193 cm^{-1} and 1142 cm^{-1} .
14
15 Furthermore, similar conclusions were drawn from the FTIR analysis of modified laponite JS
16
17 (Figure S1).
18
19
20
21



41
42 **Figure 2.** Infrared spectra of unmodified laponite XLG (black), 1H,1H,2H,2H-
43
44 perfluorooctyltriethoxysilane modified laponite (red) and 1H,1H,2H,2H-
45
46 perfluorooctyltriethoxysilane (blue).
47

48
49 To gain more insight into the bonding character after the modification process,
50
51 thermogravimetric analysis was used to determine the amount of silane covalently anchored to
52
53 the laponite nanodiscs. Figure 3 shows the TGA curves before and after the laponite
54
55 modification with the silane reagent. The samples were subjected to continuous heating up to
56
57
58
59
60

1
2
3 700 °C, ramped with 10 °C/min. The thermogram of modified XLG laponite exhibited three
4
5 main decomposition regions. The first region ranged from room temperature to 250 °C, which
6
7 likely corresponds to water elimination and hydroxyl decomposition. The third region ranged
8
9 from 550 °C to 700 °C, where no major processes seem to occur. The intermediate, second
10
11 region between 250 °C and 550 °C, is the range where the thermal decomposition of the
12
13 covalently attached silane moiety was expected, and was thus considered for the quantification of
14
15 the laponite modification. Remarkably, a high degree of organic functionalization was achieved
16
17 with circa 60% of the overall particle weight. This high degree of functionalization is of great
18
19 interest as it may induce strong omniphobic characteristics provided by these particles, which
20
21 will be explained later in this study. The observed silane modification ratio greatly outperforms
22
23 similar modification of other range of laponite (RD nanodiscs) previously reported in the
24
25 literature, which reached approximately 13% after functionalization with perfluorooctylsilane.²²
26
27 Also further similar studies with various silane groups for laponite functionalization with diverse
28
29 aims showed organic functionalization ranging from 5 to 17% of the overall weight.^{23,24,27}
30
31 However, omniphobic functionalization of SiO₂²⁸ or TiO₂^{29,30} nanoparticles in a similar approach
32
33 to the work described in this study has yielded functionalization of approximately 10% and 20%
34
35 of the particle weight. The large physical surface of laponite of about 900 m²/g,³¹ the strong
36
37 nucleophilic character of laponite XLG nanodiscs, resulting from a large concentration of
38
39 hydroxyl and oxygen atoms, and the more severe synthesis conditions employed in this study
40
41 may serve as explanation for our results. Thermal gravimetric analysis of unmodified laponite
42
43 XLG clay expectedly did not show any silane-related feature. A weight loss of 10% was detected
44
45 upon heating of the unmodified laponite to 150 °C, which is mainly due to the presence of water
46
47 molecules. The lower weight loss detected for functionalized laponite in the same temperature
48
49
50
51
52
53
54
55
56
57
58
59
60

range anticipates hydrophobic character of those. Similar silanization of laponite JS (Figure S2) was performed and showed rather modest values of about 20% of functionalization. This finding suggests that the absence of pyrophosphate groups in laponite XLG is favorable for a quantitative modification of laponites.

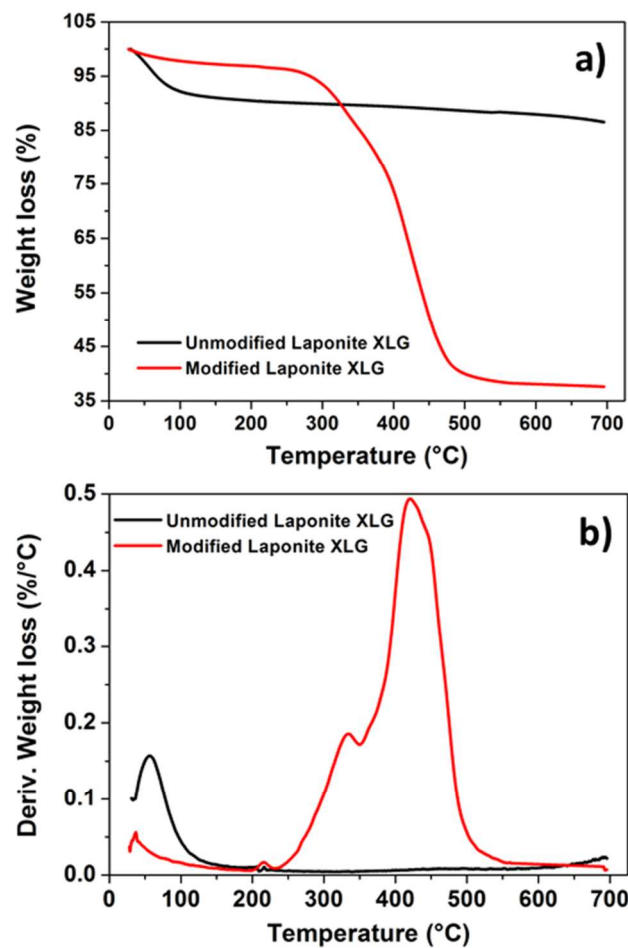


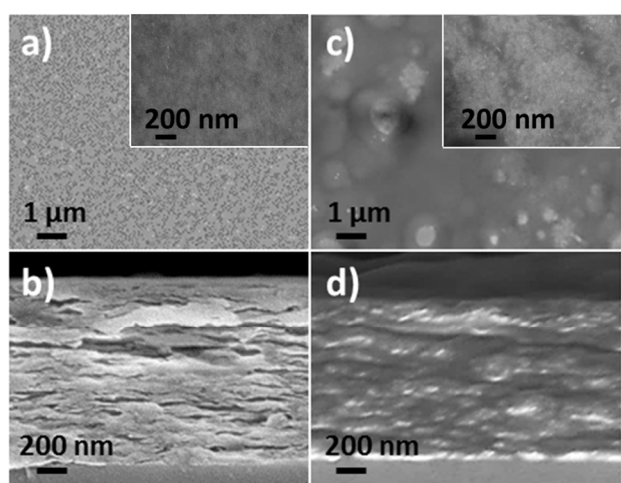
Figure 3. a) Thermogravimetric analysis (TGA) of laponite XLG (black), and laponite XLG, modified with 1H,1H,2H,2H-perfluorooctyltriethoxysilane (red); b) first derivative of TGA curves showing changes of weight loss in the unmodified and modified laponites.

Unmodified and multifunctional laponite coatings

1
2
3 Besides the interesting results observed when laponites are stabilized as colloids in a gel
4 state,^{32,33} unmodified laponites are also known as film forming agents with excellent antistatic
5 and permeation barrier properties. Examples of laponite films in the literature include those
6 obtained after slow evaporation of laponite in water dispersions^{16,18} or after their addition to resin
7 emulsion binders.^{22,34,35} Here, the 4% (w/v) ethanolic-aqueous gel mixture obtained after the
8 synthesis of modified XLG laponite nanoparticles was processed into films using a bar-coating
9 application with a 100 μm cylindrical bar. The resulting films were hydrophobic with a contact
10 angle of 110°. However, the obtained perfluoroalkylsilane-modified laponite films were not
11 electrically conductive. The most likely reason is the quantitative functionalization of the
12 laponite clays, which blocks the electrical charge transport and distorts the interlinked and
13 overlapping arrangement of the laponite platelets.^{20,31} In order to overcome this limitation, which
14 has a negative impact on the dust-repellent functionality, formulations were made which include
15 both electrically conductive unmodified laponite and insulating perfluoroalkylsilane-modified
16 laponite. Indeed, blending with unmodified laponites may not only ensure electrical conductivity
17 and dust-repellence, but may also pave the way to the formation of films with excellent quality.
18 Finally, a suitable multifunctional composition was found after mixing unmodified laponites
19 dispersion and perfluoroalkylsilane-modified laponite XLG 4% (w/v) in a 7:3 ratio.
20
21
22
23
24
25
26
27
28
29
30
31
32
33
34
35
36
37
38
39
40
41
42
43
44

45 The obtained films were further characterized regarding their morphology, optical properties,
46 dust-repellence and omniphobicity performance, and mechanical behavior. Figure 4 displays
47 representative top-view and cross-sectional FESEM micrographs of the films constituted by
48 mixtures of unmodified and multifunctional laponites. The films obtained from unmodified XLG
49 and JS laponites showed no significant microscale features in top-view (Figure 4a) and a layered
50 stacking structure in cross-section (Figure 4b). A structure conformation in which some layer
51
52
53
54
55
56
57
58
59
60

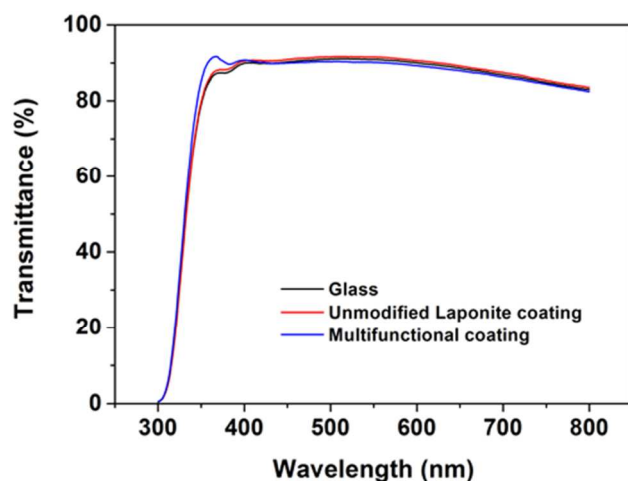
1
2
3 stacking may be also inferred, although less obviously than in the unmodified laponite film, was
4
5 also detected for the multifunctional films (Figure 4d). Furthermore, some microscale features at
6
7 the surface were detected (Figure 4c). Note that films deposited from suspensions of only
8
9 functionalized laponite XLG showed larger density of microscale features and higher porosity
10
11 (Figure S3), likely resulting from swelling and bubble formation occurred during ethanol
12
13 evaporation from the laponite dispersion.
14
15
16
17
18



36
37 **Figure 4.** FE-SEM micrographs of unmodified XLG and JS laponites in a 7:3 mixture after
38 coating in a) top view and b) cross-sectional view. FE-SEM micrographs of the multifunctional
39 coating (mixture of unmodified and modified laponites) in c) top view and d) cross-sectional
40
41 view.
42
43
44
45

46
47 Often the final applications of self-cleaning coatings require some degree of transparency (e.g.
48 aesthetics products,^{9,36} or solar cells¹²). Therefore the UV/visible light transmittance of the films
49
50 was characterized (Figure 5). Both unmodified laponites and multifunctional laponites coatings
51
52 were applied to transparent glass substrates through bar-coating and their transparency were
53
54 measured. At the first sight, no significant differences in the visible region (approx. 380 – 750
55
56
57
58
59
60

1
2
3 nm) between the two laponite coatings and the bare glass substrate were observed in
4
5 transmittance mode. However, a closer look to the spectra reveals that samples having the
6
7 multifunctional laponite coating exhibited slightly lower transmittance in the visible, but also a
8
9 significant increase in transmittance in the UV range (i.e. below 380 nm). It is worth mentioning
10
11 that samples with multifunctional coatings exhibited the lowest reflectance (Figure S4),
12
13 suggesting an alteration of the effective refractive index. The latter may be due to the different
14
15 chemical nature of the coating, but may also result from changes in the morphology. It is indeed
16
17 worth highlighting that enhanced light scattering may occur in multifunctional coatings (i.e.
18
19 micro/nanoscale morphological features) (Figure S5).
20
21
22
23
24



43 **Figure 5.** Total optical transmittance of bare glass (black), glass coated with unmodified XLG
44 and JS laponites in a 7:3 ratio (red), and glass with the multifunctional coating (blue).
45
46
47

48
49 One of the characteristics of these coatings is their capacity to perform as antistatic agents, which
50 relies on the intrinsic electrical and ionic conductivities of laponites. Therefore, the electrical
51 conductivities of unmodified and multifunctional laponite coatings were measured. Any
52
53
54
55
56
57
58
59
60 electrical contribution in the measurements that may be originated from the substrate was

avoided by applying coatings to blue PVC sheets and glass substrates. The PVC substrate is characterized as dielectric material prone to static charges. The electrical sheet resistance values are depicted at Table 1. All coated PVC substrates had a sheet resistance in the range of 10^6 and $10^7 \Omega/\square$ and the uncoated PVC substrate used as reference had a sheet resistance above $10^{13} \Omega/\square$. Note that films with sheet resistances between $10^5 \Omega/\square$ and $10^{12} \Omega/\square$ generally may allow dissipation of electrical charges within milliseconds.³⁷ Thus, both unmodified and multifunctional laponite coatings should have antistatic characteristics and may exhibit dust-repellence feature.

Table 1. Sheet resistance of bare and laponite-coated substrates.

Coating	PVC (Ω/\square)	Glass (Ω/\square)
Bare substrate	$> 5 \times 10^{13}$	$2.3 \pm 0.3 \times 10^{10}$
Unmodified laponites	$9.0 \pm 1.0 \times 10^6$	$3.5 \pm 0.5 \times 10^7$
Multifunctional	$3.0 \pm 0.2 \times 10^7$	$1.2 \pm 0.1 \times 10^8$

The dust attraction test confirmed these assumptions. Figure 6-a shows photographs of bare PVC substrates and PVC substrates coated with both types of laponite mixtures, that is, the unmodified XLG:JS laponite mixture and the modified multifunctional laponite coating. The uncoated and coated samples were placed inside a box with a holed lid and carbon black dust inside. Through the orifice, air was blown into the box with a pressurized gun in order to generate a carbon black cloud inside the box. After 30 seconds of air blowing, the samples were removed and examined. The two laponite coatings (antistatic/unmodified and multifunctional) exhibited similar behavior, with only small amounts of carbon black dust remaining attached to the surface. In contrast, the bare PVC sample was significantly covered with carbon black dust.

1
2
3 These results showed that the coated samples with a lower electrical sheet resistance are more
4
5 favorable to evade dust accumulation.
6
7

8
9 The static contact angles of uncoated PVC and PVC coated with unmodified or multifunctional
10 laponites were measured as a qualitative indicator to evaluate the liquid repellence functionality
11 (Table 2). Uncoated PVC showed very oleophilic character, with modest values of contact angles
12 against organic oils, mineral oils and hexadecane. As expected from its hydrophobic polymeric
13 nature, it showed a water contact angle of 90°. The unmodified laponite coating did not improve
14 the oleophobic character of the bare PVC substrate, but a significant reduction of the water
15 contact angle was observed. The ionic nature of laponite clays increased the water affinity of the
16 coating. The multifunctional coatings, in contrast, showed contact angle values with a significant
17 improvement over both bare PVC and unmodified laponite coatings. The $-CF_2-$ and $-CF_3$ groups
18 contained in the introduced silanes enhanced the omniphobic character by reducing the surface
19 free energy, thereby increasing the static contact angle values (Table 2).^{38,39}
20
21
22
23
24
25
26
27
28
29
30
31
32
33
34
35

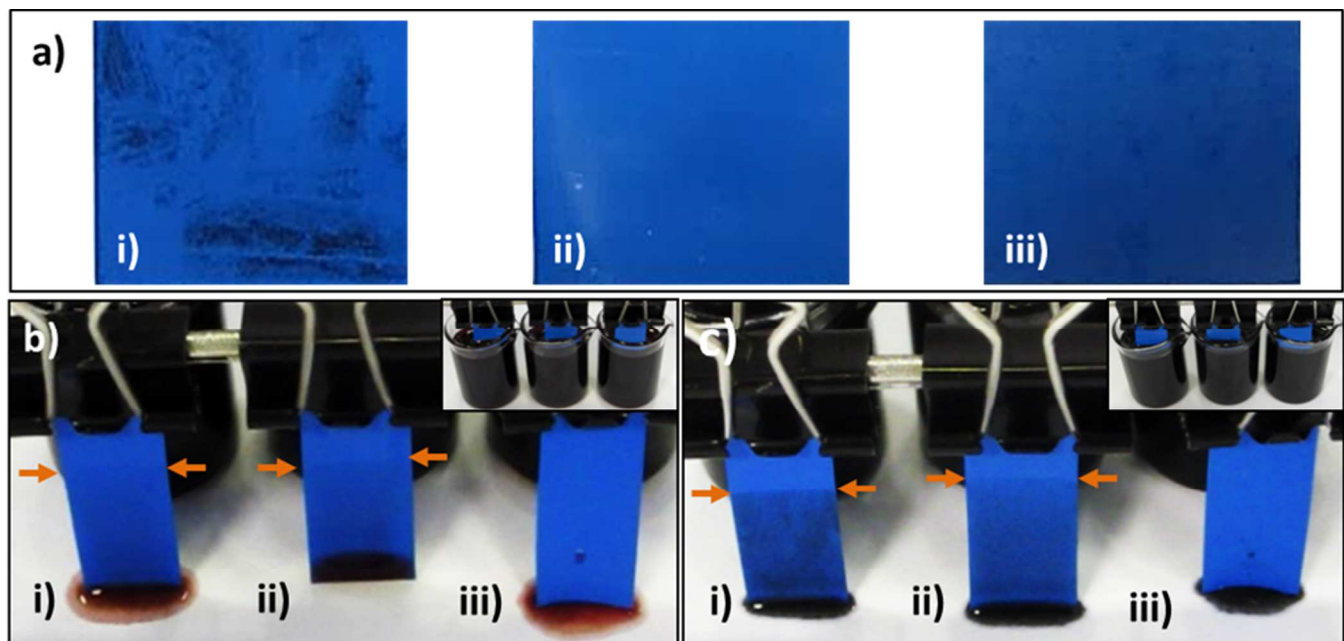
36 **Table 2.** Static contact angles observed for bare PVC, unmodified XLG and JS laponites in a 7:3
37 ratio mixture coating, and multifunctional coating (mixture of unmodified and functionalized
38 laponites) for various liquids.
39
40
41
42
43

Liquid	Bare PVC	Unmodified laponites	Multifunctional coating
Water	90±1°	19±1°	106±1°
PAO 9	28±2°	27±1°	93±2°
Mineral Oil (GIII)	26±1°	25±3°	88±3°
Hexadecane	25±2°	<10°	64±1°

1
2
3 The results show that good repellence against polar solvents, such as water, and non-polar and
4 organic oils, such as polyalphaolefin (PAO 9), is achieved with the multifunctional coatings. For
5 further organic solvents, such as hexadecane, the static contact angles were more discrete. This
6 can be explained by the low surface tension of hexadecane (27.4 mN/m) versus water (72.8
7 mN/m).⁴⁰ However, the contact angles for hexadecane obtained from the multifunctional
8 modified laponite coatings are in good agreement with literature values obtained from
9 fluorinated bulk materials,⁴¹ or even significantly higher than those obtained by other approaches
10 with non-hierarchical morphology surfaces modified with low surface energy materials,^{40,42,43} or
11 infused liquid surfaces.⁴⁴ The evidence shows that the presence of unmodified laponites in the
12 multifunctional coating formulation has no negative impact on the contact angles. This behavior
13 is further supported by the surface energy measured for the different surfaces and coatings. As
14 expected, the multifunctional coating showed the lowest value (12.05 mN/m) in contrast to the
15 antistatic laponite coating (64.08 mN/m) and bare PVC (39.03 mN/m) values. Further data can
16 be found in Table S1.

17
18
19
20
21
22
23
24
25
26
27
28
29
30
31
32
33
34
35
36
37 To assess the self-cleaning performance of both laponite coatings, the bare PVC sample and the
38 two coated PVC samples (XLG:JS unmodified laponite and multifunctional laponite) were
39 placed in two oil tanks. The first oil tank contained tinted PAO 9 oil (Figure 6-b) and the second
40 tank mineral oil (GIII) with suspended carbon black dust in order to simulate an aged oil
41 composed of oil and solid particles (Figure 6-c). The excellent self-cleaning response of the
42 multifunctional coating when subjected to both oils can be observed in Movie S1 (tinted PAO 9
43 oil) and Movie S2 (mineral oil with carbon dust particles). Despite showing modest dynamic
44 contact angles and hysteresis results (Table S2), the surface of the multifunctional coating
45 repelled the oil and the stains within seconds, while the bare PVC and unmodified laponite
46
47
48
49
50
51
52
53
54
55
56
57
58
59
60

1
2
3 coating remained covered by oil after the test. The dust- and liquid-repellence holistic
4
5 functionalities indicate that the modified multifunctional coatings are well suitable for a use as
6
7 self-cleaning coatings, since they avoid any kind of dirt accumulation, including dust particles,
8
9 liquids of different nature and a combination thereof. This is advantageous over other systems,
10
11 where the self-cleaning concept is based exclusively on liquid repellence, by allowing water
12
13 droplets to carry the dirt off of the surface along the rolling droplet path.⁴⁵⁻⁴⁶
14
15
16
17



41 **Figure 6.** a) Dust repellence tests against carbon black powder of i) bare PVC; ii) unmodified
42 laponites mixture, and iii) multifunctional coating; b) Oil self-cleaning test of i) bare PVC; ii)
43 unmodified laponites mixture and iii) multifunctional coating; c) Oil and carbon black mixture
44 self-cleaning test of i) bare PVC; ii) unmodified laponites mixture and iii) multifunctional
45 coating. In b) and c) red arrows indicate the presence of immersion marks after being immersed
46
47
48
49
50
51
52
53
54
55
56
57
58
59
60

In order to evaluate the mechanical stability of the coatings, coated PVC samples were subjected to bending tests and their liquid-repellence behavior was investigated thereafter. As seen in Table 3, water contact angles for both coatings (unmodified XLG:JS laponite and multifunctional) remained unaffected after the tests. However, the coating was studied more in depth by electron microscopy after the bending tests and the damage resulting from bending was evaluated. Figure 7 shows that the unmodified laponite coating gained clear fissures. In contrast, the multifunctional coating did not show any fissures, but some folding lines along the bending axis. It is clear that the less ordered stacking character of the multifunctional coating, as seen in the cross-sectional micrograph in Figure 4, prevents fracturing during manipulation, thereby increasing the plasticity and temporal stability of the coating.

Table 3. Water static angle values for unmodified laponites and multifunctional coatings over a PVC flexible substrate after a series of bending tests.

Coating	0 bending cycles	2 bending cycles	20 bending cycles	100 bending cycles
Unmodified laponites	$20 \pm 1^\circ$	$19 \pm 2^\circ$	$20 \pm 1^\circ$	$20 \pm 2^\circ$
Multifunctional	$106 \pm 1^\circ$	$108 \pm 2^\circ$	$107 \pm 2^\circ$	$105 \pm 3^\circ$

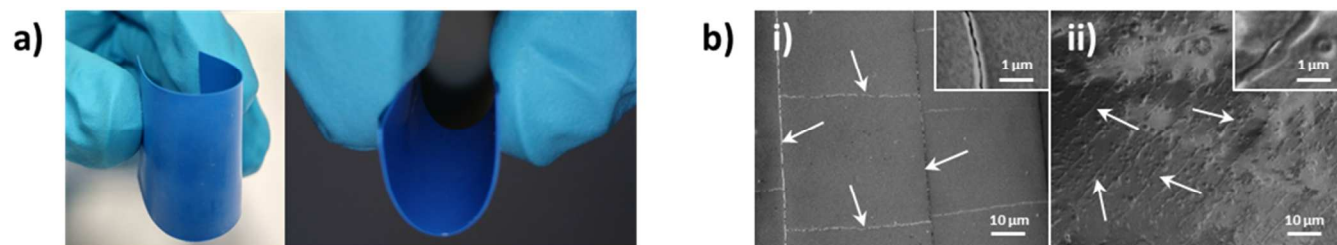


Figure 7. a) Bending of a blue PVC flexible substrate with a 100 μm thick multifunctional coating. b) FE-SEM images after 100 bending cycles of: i) unmodified laponite showing fissures and ii) multifunctional coatings showing folding lines.

4. CONCLUSIONS

Innovative coatings with dual-action, anti-dust accumulation and liquid repellence, are proposed for a holistic approach with a triple active self-cleaning response against liquids, solids and liquid-solid mixtures. We demonstrated a pathway to tune the hydrophilic laponite into omniphobic films simply by blending raw laponite particles with a certain amount of a highly perfluoroalkylsilanized laponite clay (e.g. 7:3). The resulting mixture allowed us to deposit multifunctional coatings with holistic self-cleaning functionality based on omniphobicity and reduced dust-attraction properties. This is a step beyond classical omniphobic approaches, where only repellence towards liquids has been shown. Employment of a low processing temperature and a water-based formulation have been successfully demonstrated in order to obtain such holistic self-cleaning coatings, which opens wide opportunities for applications in numerous sectors, including electronics, automotive, architecture, furniture protection or decoration.

ASSOCIATED CONTENT

Supporting Information available.

Additional information regarding Infrared Spectra of laponite JS and perfluorinated-modified laponite JS, Thermogravimetry Analysis of laponite JS and perfluorinated-modified laponite JS, FE-SEM, Spectrophotometric data of fabricated films, measured data of surface free energy, dynamic and hysteresis contact angles and 2 video files showing the self-cleaning performance of multifunctional coatings against different oils and carbon black mixtures are included.

1
2
3 This material is available free of charge via the Internet at <http://pubs.acs.org>.
4
5
6
7

8
9 **AUTHOR INFORMATION**

10
11 **Corresponding Author**

12
13
14 * IK4-CIDETEC, Parque Tecnológico de San Sebastián, Paseo Miramón, 196, 20014 Donostia -
15
16 San Sebastián, Spain.

17
18
19
20 E-mail: jpalenzuela@cidetec.es
21
22

23
24 **Author Contributions**

25
26 The manuscript was written through contributions of all authors. All authors have given approval
27
28 to the final version of the manuscript.
29
30

31
32 **Notes**

33
34 The authors declare no competing financial interest.
35
36
37
38
39
40

41
42 **ACKNOWLEDGMENT**

43
44 This work was financially supported by the Basque Government under the ELKARTEK 2016
45
46 program contract no. KK-2016/00093 (FRONTIERS). M.K. acknowledges financial support
47
48 from the Spanish Ministry of Economy and Competitiveness (MINECO) (MAT2016-77393-R,
49
50 including FEDER funds, EU) and I.A. the support from the Doctoral Programme of the
51
52 Department of Education, Linguistic Policy and Culture of the Basque Government. Also, the
53
54 authors would like to acknowledge Dr Ivet Kosta for helping in FESEM image characterization.
55
56
57
58
59
60

REFERENCES

- 1 Tian, X.; Verho, T.; R. Ras, R. H. A. Moving Superhydrophobic Surfaces Toward Real-
2 World Applications. *Science*, **2016**, 352, 142-143.
- 3
4
5
6
7
8
9
10
11
12
13
14
15
16
17
18
19
20
21
22
23
24
25
26
27
28
29
30
31
32
33
34
35
36
37
38
39
40
41
42
43
44
45
46
47
48
49
50
51
52
53
54
55
56
57
58
59
60
2
3
4
5
6
7
8
9
10
11
12
13
14
15
16
17
18
19
20
21
22
23
24
25
26
27
28
29
30
31
32
33
34
35
36
37
38
39
40
41
42
43
44
45
46
47
48
49
50
51
52
53
54
55
56
57
58
59
60
- 2 Wang, S.; Liu, K.; Yao, X.; Jiang, L. Bioinspired Surfaces with Superwettability: New
3 Insight on Theory, Design, and Applications. *Chem. Rev.*, **2015**, 115, 8230-8293.
- 4 Samaha, M. A.; Gad-el-Hak, M. Polymeric Slippery Coatings: Nature and Applications.
5 *Polymers*, **2014**, 6, 1266-1311.
- 6 Hensel, R.; Neinhuis, C.; Werner, C. The Springtail Cuticle as a Blueprint for
7 Omniphobic Surfaces. *Chem. Soc. Rev.*, **2016**, 45, 323-341.
- 8 Wu, L. Y. L.; Shao, Q.; Wang, X. C.; Zheng, H. Y.; Wong, C. C. Hierarchical Structured
9 Sol-Gel Coating by Laser Textured Template Imprinting for Surface Superhydrophobicity. *Soft*
10 *Matter*, **2012**, 8, 6232-6238.
- 11 Yu, M.; Chen, S.; Zhang, B.; Qiu, D.; Cui, S. Why a Lotus-like Superhydrophobic
12 Surface is Self-Cleaning? An Explanation from Surface Force Measurements and Analysis.
13 *Langmuir*, **2014**, 30, 13615-13621.
- 14 Lai, Y.; Tang, Y.; Gong, J.; Gong, D.; Chi, L.; Lin, C.; Chen, Z. Transparent
15 Superhydrophobic/Superhydrophilic TiO₂-Based Coatings for Self-Cleaning and Anti-Fogging.
16 *J. Mater. Chem.*, **2012**, 22, 7420-7426.
- 17 Bhushan, B. Biomimetics Inspired Surfaces for Drag Reduction and
18 Oleophobicity/philicity. *Beilstein J. Nanotechnol.*, **2011**, 2, 66-84.

1
2
3 9 Martin, S.; Bhushan, B. Transparent, Wear-Resistant, Superhydrophobic and
4 Superoleophobic Poly(dimethylsiloxane) (PDMS) Surfaces. *J. Colloid Interface Sci.*, **2017**, 488,
5 118-126.
6
7
8

9
10
11 10 Xiong, L.; Kendrick, L.; Heusser, H.; Webb, J. C.; Sparks, B. J.; Goetz, J. T.; Guo, W.;
12 Stafford, C. M.; Blanton, M. D.; Nazarenko, S.; Patton, D. L. Spray-Deposition and
13 Photopolymerization of Organic-Inorganic Thiol-ene Resins for Fabrication of
14 Superamphiphobic Surfaces. *ACS Appl. Mater. Interfaces*, **2014**, 6, 10763-10774.
15
16
17
18

19
20
21 11 Deng, X.; Mammen, L.; Butt, H-J.; Vollmer, D. Candle Soot as a Template for a
22 Transparent Robust Superamphiphobic Coating, *Science*, **2012**, 335, 67-70.
23
24
25
26

27 12 Narushima, D.; Takanohashi, H.; Hirose, J.; Ogawa, S. Antistatic Effect of Power-
28 Enhancement Coating for Photovoltaic Modules. *Proc. SPIE*, **2011**, 8112, 811208-1.
29
30
31
32

33 13 Baytekin, H. T.; Baytekin, B.; Hermans, T. M.; Kowalczyk, B.; Grzybowski, B. A.
34 Control of Surface Changes by Radicals as a Principle of Antistatic Polymers Protecting
35 Electronic Circuitry. *Science*, **2013**, 341, 1368-1371.
36
37
38
39

40 14 Greason, W. D. Review of the Effect of Electrostatic Discharge and Protection
41 Techniques for Electronic Systems. *IEEE Trans. Ind. Appl.*, **1987**, IA-23, 205-216.
42
43
44
45

46 15 Gibson, N. Static Electricity – an Industrial Hazard under Control? *J. Electrostat.*, **1997**, 40-
47 41, 21-30.
48
49
50

51 16 Lezhnina, M. M.; Grewe, T.; Stoehr, H.; Kynast, U. Laponite Blue: Dissolving the
52 Insoluble. *Angew. Chem., Int. Ed.* **2012**, 51, 10652-10655.
53
54
55
56
57
58
59
60

1
2
3 17 Nobel, M. L.; Picken, S. J.; Mendes, E. Waterborne Nanocomposite Resins for
4 Automotive Coatings Applications. *Prog. Org. Coat.*, **2007**, 58, 96-104.
5
6

7
8
9 18 Luyer, C. L.; Lou, L.; Bovier, C.; Plenet, J. C.; Dumas, J. G.; Mugnier, J. A Thick Sol-
10 Gel Inorganic Layer for Optical Planar Waveguide Applications. *Opt. Mater.*, **2001**, 18, 211-217.
11
12

13
14 19 Wu W.; Dong, Z.; He, J.; Yu, J.; Zhang, J. Transparent Cellulose/Laponite
15 Nanocomposite Films. *J. Mater. Sci.*, **2016**, 51, 4125-4133.
16
17

18
19
20 20 Li, Y.; Schulz, J.; Grunlan, J. C. Polyelectrolyte/Nanosilicate Thin-Film Assemblies:
21 Influence of pH on Growth, Mechanical Behavior, and Flammability. *ACS Appl. Mater.*
22 *Interfaces*, **2009**, 1, 2338-2347.
23
24
25

26
27
28 21 Santana, I.; Pepe, A.; Schreiner, W.; Pellice, S.; Ceré, S. Hybrid Sol-Gel Coatings
29 Containing Clay Nanoparticles for Corrosion Protection of Mild Steel. *Electrochim. Acta*, **2016**,
30 203, 396-403.
31
32
33

34
35
36 22 Swartz, N. A.; Price, C. A.; Clare, T. L. Minimizing Corrosion of Outdoor Metalworks
37 Using Dispersed Chemically Stabilized Nanoclays in Polyvinylidene Fluoride Latex Coatings.
38 *ACS Omega*, **2016**, 1, 138-147.
39
40
41

42
43
44 23 Wu, Y.; Guo, R.; Wen, S.; Shen, M.; Zhu, M.; Wang, J.; Shi, X. Folic Acid-Modified
45 Laponite Nanodiscs for Targeted Anticancer Drug Delivery. *J. Mater. Chem. B*, **2014**, 2, 7410-
46 7418.
47
48
49

50
51
52 24 Wheeler P. A.; Wang, J.; Baker, J.; Mathias L. J. Synthesis and Characterization of
53 Covalently Functionalized Laponite. *Chem. Mater.*, **2005**, 17, 3012-3018.
54
55
56
57
58
59
60

1
2
3 25 Cummins, H. Z. Liquid, Glass, Gel: The Phases of Colloidal Laponite. *J. Non-Cryst.*
4
5
6 *Solids*, **2007**, 353, 3891-3905.

7
8
9 26 Fatnassi, M.; Solterbeck, C.-H.; Es-Souni, M. Clay Nanomaterial Thin Film Electrodes
10
11 for Electrochemical Energy Storage Applications. *RSC Adv.*, **2014**, 4, 46976-46979.

12
13
14 27 Herrera, N.; Letoffe, J_M.; Putaux, J-L.; David, L.; Bourgeat-Lami, E. Aqueous
15
16 Dispersions of Silane-Functionalized Laponite Clay Platelets. A First Step toward the
17
18 Elaboration of Water-Based Polymer/Clay Nanocomposites. *Langmuir*, **2004**, 20, 1564-1571.

19
20
21 28 Livi, S.; Giannelis, E. P. An Improved Process for the Surface Modification of SiO₂
22
23
24 Nanoparticles. *Green Chem.*, **2012**, 14, 3013-3015.

25
26
27 29 Pazokifard, S.; Mirabedini, S. M.; Esfandeh, M; Farrokhpay, S. Structure and Properties
28
29
30 of Fluoroalkylsilane Treated Nano-Titania, *Chemeca 2011 Proc.*, **2011**, 1-10.

31
32
33 30 Chen, L.; Guo, Z.; Liu, W. Biomimetic Multi-Functional Superamphiphobic FOTS-TiO₂
34
35
36 Particles beyond Lotus Leaf. *ACS Appl. Mater. Interfaces*. **2016**, 8, 27188-27198.

37
38
39 31 BYK Additives & Instruments. Laponite Technical Brochure,
40
41 [https://www.byk.com/fileadmin/byk/additives/product_groups/rheology/former_rockwood_addit](https://www.byk.com/fileadmin/byk/additives/product_groups/rheology/former_rockwood_additives/technical_brochures/BYK_B-RI21_LAPONITE_EN.pdf)
42
43
44 [ives/technical_brochures/BYK_B-RI21_LAPONITE_EN.pdf](https://www.byk.com/fileadmin/byk/additives/product_groups/rheology/former_rockwood_additives/technical_brochures/BYK_B-RI21_LAPONITE_EN.pdf), (accessed August 2017).

45
46
47 32 Ruzicka, B.; Zaccarelli, E.; Zulian, L.; Angelini, R.; Sztucki, M.; Moussaïd, A.; T.
48
49
50 Narayanan, T.; Sciortino, F. Observation of Empty Liquids and Equilibrium Gels in a Colloidal
51
52
53 Clay. *Nat. Mater.*, **2011**, 10, 56-60.

1
2
3 33 Wang, Q.; Mynar, J. L.; Yoshida, M.; Lee, E.; Lee, M.; Okuro, K.; Kinbara, K.; Aida, T.
4 High-Water-Content Mouldable Hydrogels by Mixing Clay and a Dendritic Molecular Binder.
5
6 *Nature*, **2010**, 463, 339-343.
7
8

9
10
11 34 Zengeni, E.; Hatmann, P. C.; Pasch, H. Encapsulation of Clay by Ad-Miniemulsion
12 Polymerization: The Influence of Clay Size and Modifier Reactivity on Latex Morphology and
13 Physical Properties. *ACS Appl. Mater. Interfaces*, **2012**, 4, 6957-6968.
14
15

16
17
18 35 Wheeler, P. A.; Wang, J.; Mathias, L. J. Poly(methyl methacrylate)/Laponite
19 Nanocomposites: Exploring Covalent and Ionic Clay Modifications. *Chem. Mater.*, **2006**, 18,
20 3937-3945.
21
22
23

24
25
26
27 36 Brown, P. S.; Bhushan, B. Mechanically Durable, Superomniphobic Coatings Prepared
28 by Layer-by-Layer Technique for Self-Cleaning and Anti-Smudge. *J. Colloid Interface Sci.*,
29 **2015**, 456, 210-218.
30
31
32

33
34
35 37 Craftech Industries. [http://info.craftechind.com/blog/an-introduction-to-anti-static-](http://info.craftechind.com/blog/an-introduction-to-anti-static-dissipative-and-conductive-plastics)
36 [dissipative-and-conductive-plastics](http://info.craftechind.com/blog/an-introduction-to-anti-static-dissipative-and-conductive-plastics) (accessed August 2017).
37
38

39
40
41 38 Chaudhury, M. K.; Whiteside, G. M.; Correlation Between Surface Free Energy and
42 Surface Constitution. *Science*. **1992**, 255, 1230-1232.
43
44

45
46 39 Katasho, Y.; Liang, Y.; Murata, S.; Fukunaka, Y.; Matsuoka, T.; Takahashi, S.
47 Mechanisms for Enhanced Hydrophobic by Atomic-Scale Roughness. *Sci. Rep.*, **2015**, 5, 13790.
48 DOI: 10.1038/srep13790.
49
50

51
52
53
54 40 Wang, L.; McCarthy, T. J. Covalently Attached Liquids: Instant Omniphobic Surfaces
55 with Unprecedented Repellency. *Angew. Chem., Int. Ed.* **2016**, 55, 244-248.
56
57
58
59
60

1
2
3 41 Rabnawaz, M.; Liu, G. Graft-Copolymer-Based Approach to Clear, Durable, and Anti-
4 Smudge Polyurethane Coatings. *Angew. Chem., Int. Ed.* **2015**, 54, 6516-6520.
5
6

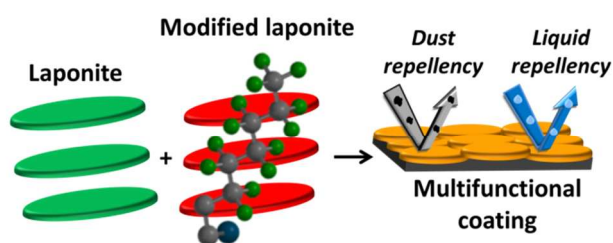
7
8
9 42 Rabnawaz, M.; Liu, G.; Hu, H. Fluorine-Free Anti-Smudge Polyurethane Coatings.
10 *Angew. Chem., Int. Ed.* **2015**, 54, 12722-12727.
11
12

13
14 43 Chen, W.; Fadeev, A. Y.; Hsieh, M. C.; Öner, D.; Youngblood, J.; McCarthy, T. J.
15 Ultrahydrophobic and Ultralyophobic Surfaces: Some Comments and Examples. *Langmuir*,
16 **1999**, 15, 3395-3399.
17
18
19

20
21
22 44 Miranda, D. F.; Urata, C.; Mashed, B.; Dunderdale, G. J.; Yagihashi, M.; Hozumi, A.;
23 Physically and Chemically Stable Ionic Liquid-Infused Textured Surfaces Showing Excellent
24 Dynamic Omniphobicity. *APL Mater*, **2014**, 2, 056108. DOI: 10.1063/1.4876636.
25
26
27

28
29
30 45 Nine, Md J.; Cole, M. A.; Johnson, L.; Tran, D. N. H.; Losic, D. Robust
31 Superhydrophobic Graphene-Based Composite Coatings with Self-Cleaning and Corrosion
32 Barrier Properties. *ACS Appl. Mater. Interfaces*, **2015**, 7, 28482-28493.
33
34
35

36
37
38 46 Yan, W.; Liu, H.; Chen, T.; Sun, Q.; Zhu, W. Fast and Low-Cost Method to Fabricate
39 Large-Area Superhydrophobic Surface on Steel Substrate with Anticorrosion and Anti-Icing
40 Properties. *J. Vac. Sci. Technol. A*, **2016**, 34, 041401-1. DOI: 10.1116/1.4953031.
41
42
43
44
45
46
47
48
49



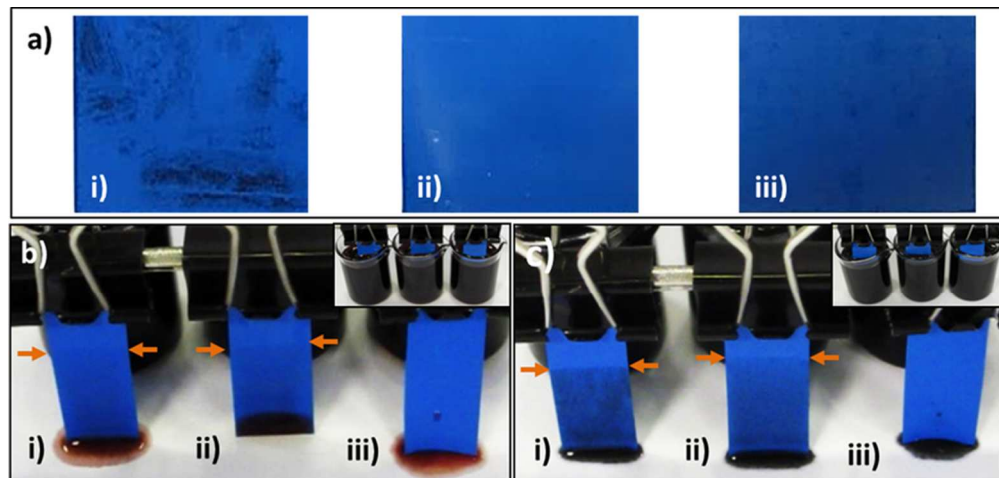


Figure 6. a) Dust repellence tests against carbon black powder of i) bare PVC; ii) unmodified laponites mixture, and iii) multifunctional coating; b) Oil self-cleaning test of i) bare PVC; ii) unmodified laponites mixture and iii) multifunctional coating; c) Oil and carbon black mixture self-cleaning test of i) bare PVC; ii) unmodified laponites mixture and iii) multifunctional coating. In b) and c) red arrows indicate the presence of immersion marks after being immersed in the oil tanks.

81x38mm (300 x 300 DPI)

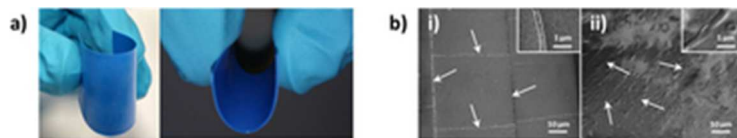
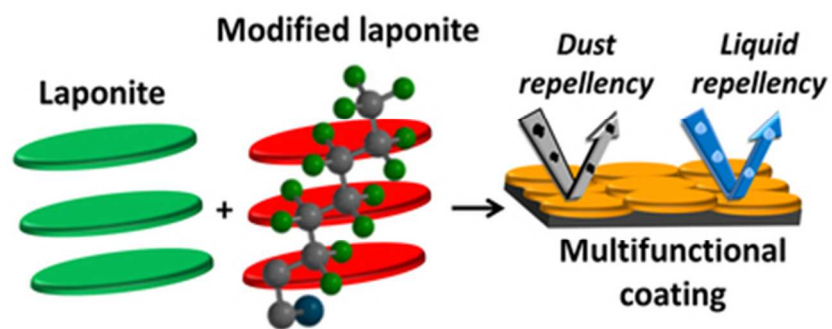


Figure 7. a) Bending of a blue PVC flexible substrate with a 100 μm thick multifunctional coating. b) FE-SEM images after 100 bending cycles of: i) unmodified laponite showing fissures and ii) multifunctional coatings showing folding lines.

31x5mm (300 x 300 DPI)



35x15mm (300 x 300 DPI)